Electronic Supplementary Information

Li_2O-B_2O_3-GeO_2 glass as a high performance anode material for rechargeable lithium-ion batteries

Seung Ho Choi,[a] Seung Jong Lee,[b] Hye Jin Kim,[b,c] Seung Bin Park,[a,*] Jang Wook Choi[c*]

[a]Department of Chemical and Biomolecular Engineering, Korea Advanced Institute of Science and Technology (KAIST), Daehakro 291, Yuseong-gu, Daejeon 34141, Republic of Korea.

[b]Graduate School of Energy, Environment, Water, and Sustainability (EEWS), Korea Advanced Institute of Science and Technology (KAIST), Daehakro 291, Yuseong-gu, Daejeon 34141, Republic of Korea.

[c]School of Chemical and Biological Engineering and Institute of Chemical Processes, Seoul National University, 1 Gwanak-ro, Gwanak-gu, Seoul 08826, Republic of Korea

Corresponding authors: E-mail: SeungBinPark@kaist.ac.kr, jangwookchoi@snu.ac.kr

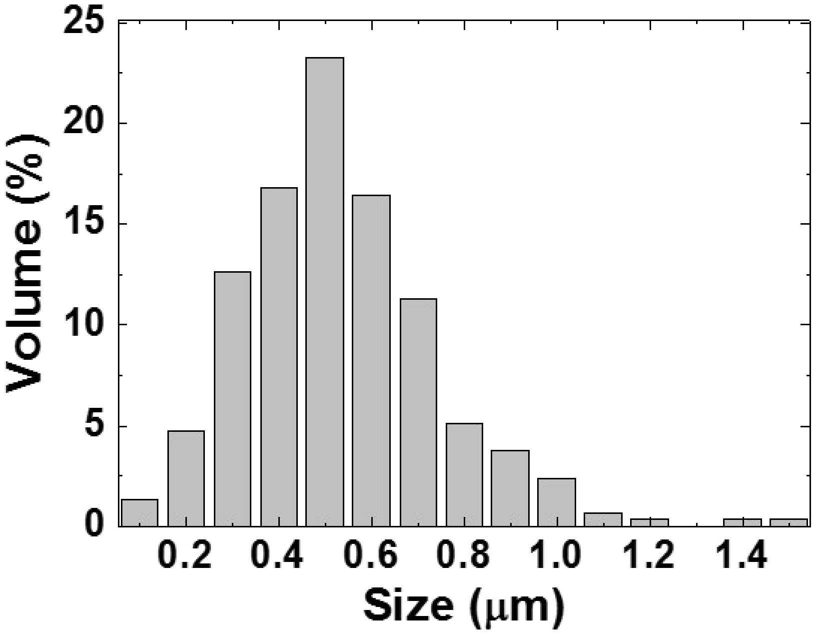

Fig. S1 Size distribution of the LBGO glass powder from low magnification SEM analysis.

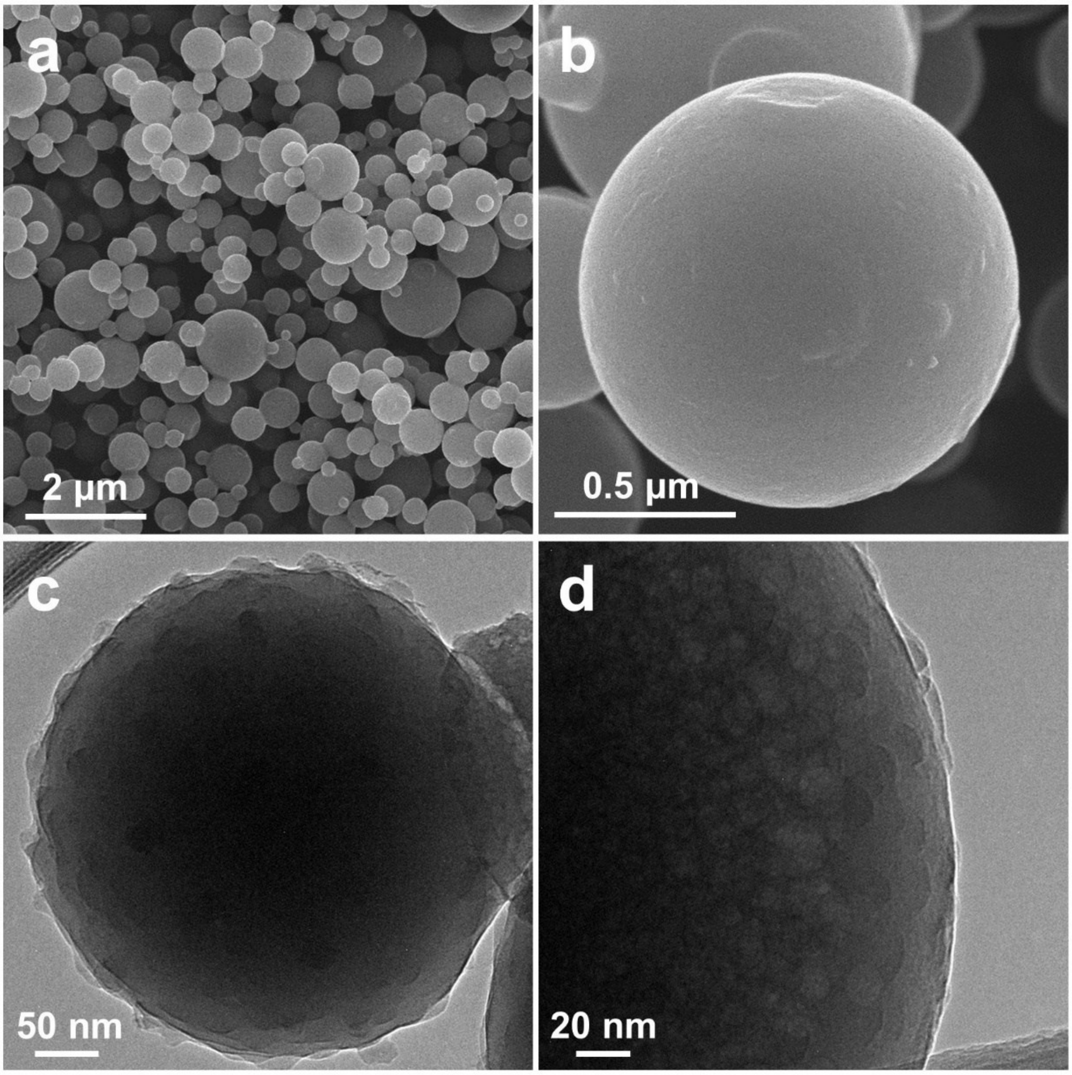

Fig. S2 Morphologies of LBO glass prepared by one-pot spray pyrolysis. (a,b) SEM images. (c,d) TEM images.

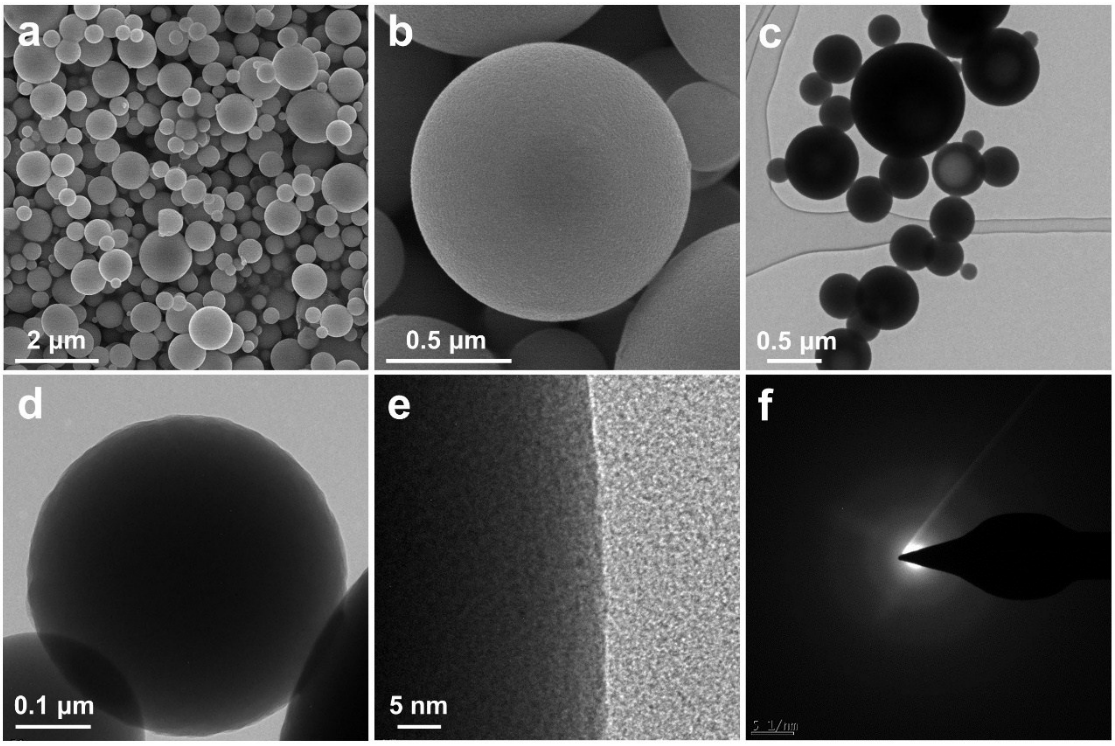

Fig. S3 Morphologies of GeO_2 powders prepared by one-pot spray pyrolysis. (a,b) SEM images. (c,d) TEM images. (e) HR-TEM image. (f) SAED pattern.

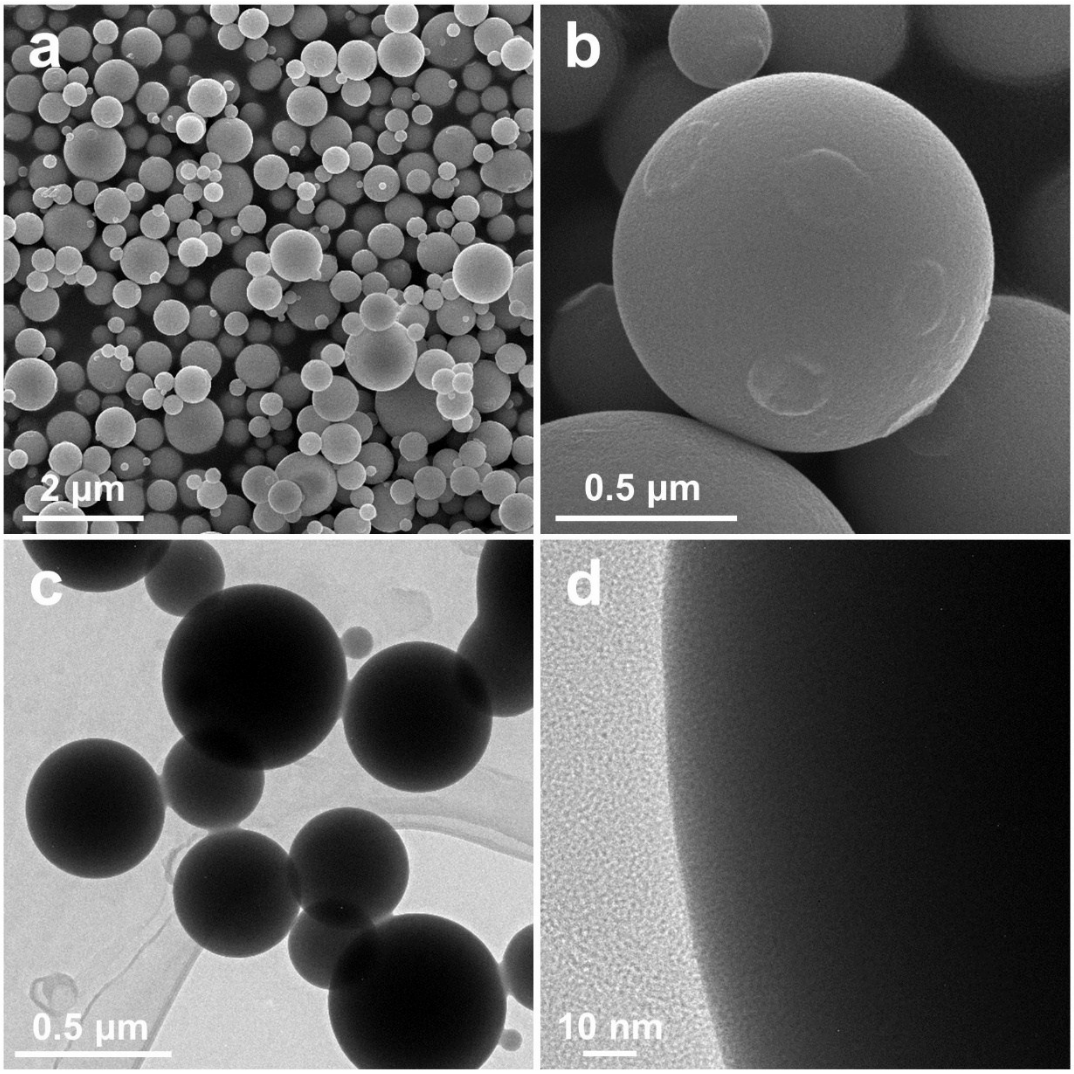

Fig. S4 Morphologies of Ge-rich LBGO glass with a molar ratio of Li_2O : B_2O_3 : GeO_2 = 1 : 2 : 4. (a,b) SEM images. (c,d) TEM images.

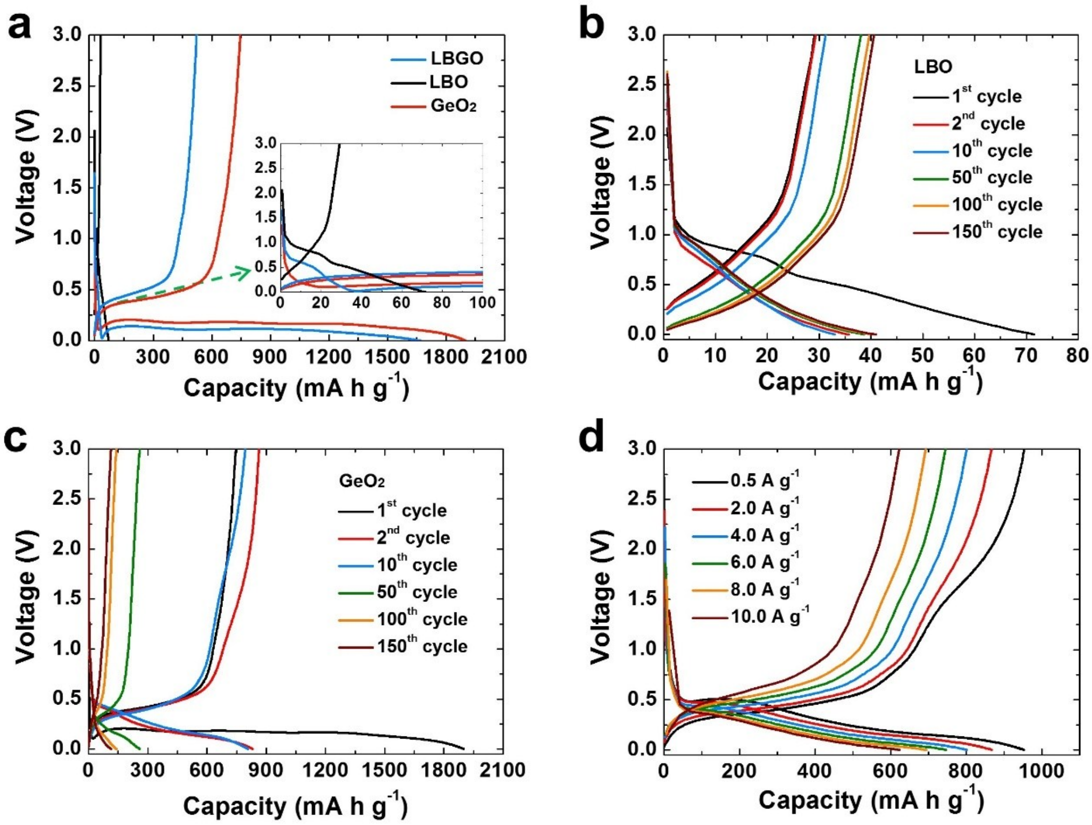

Fig. S5 Charge-discharging profiles during cycling. (a) The first charge-discharge profiles of the LBGO, LBO, and GeO_2 electrodes. Charge-discharge profiles of (b) the LBO glass and (c) the GeO_2 electrodes during cycling at a constant current density of 1 A g^{-1}. (d) Charge-discharge profiles of the LBGO glass electrode at different current densities.

Table S1. Comparison of the electrochemical performance of Li_2O-B_2O_3-GeO_2 electrode with that of reported glass materials.

Typical examples	Synthetic method	Current density (mA g^{-1})	Reversible capacity (mA h g^{-1})/ cycle number	Reference
SnO-P_2O_5 glass	solid-state and quenching	2.4 (mA cm^{-2})	540/50	28
1.5B_2O_3–SnO_x/CNFs	electrospinnin g	200 2000	670.2/100 300.2/-	29
SnB_2O_4 glass	solid-state and quenching	0.1 (mA cm^{-2})	525/40	30
$Sn_2P_2O_7$ nanodisk	quenching hydrothermal	350	547/220	45
SnO_2–B_2O_3 core–shell nanocomposite	molten-salt decomposition	156	537/100	46
SnO/P_2O_5 (67/33mol%)	melt–quenching technique	1.0 (mA cm^{-2})	356/20	47
GeO_2 glass	solid-state and quenching	134	310/30	48
GeS_2 glass	solid-state and quenching	134	414.8/30	48
Li_2O-B_2O_3-GeO_2 glass	spray pyrolysis	1000	827.6/150	this work
		10000	623	

28 H. Yamauchi, G. Park, T. Nagakane, T. Honma, T. Komatsu, T. Sakai and A. Sakamoto, *J. Electrochem. Soc.*, 2013, **160**, A1725–A1730.

29 Q. Li, J. L. Lan, Y. Liu, Y. Yu and X. Yang, *RSC Adv.*, 2015, **5**, 89099–89104.

30 C. Gejke, L. Börjesson and K. Edström, *Electrochem. Commun.*, 2003, **5**, 27–31.

45 S. Lee and J. Cho, *Chem. Commun.*, 2010, **46**, 2444–2446.

46 G. Xia, N. Li, D. Li, R. Liu, N. Xiao and D. Tian, *Mater. Lett.* 2012, **79**, 58–60.

47 A. Hayashi, T. Konishi, K. Tadanaga, T. Minami and M. Tatsumisago, *J. Non-Crystalline Solids*, 2004, **345&346**, 478–483.

48 Y. Kim, H. Hwang, K. Lawler, S. W. Martin and J. Cho, *Electrochim. Acta*, 2008, **53**, 5058–5064.

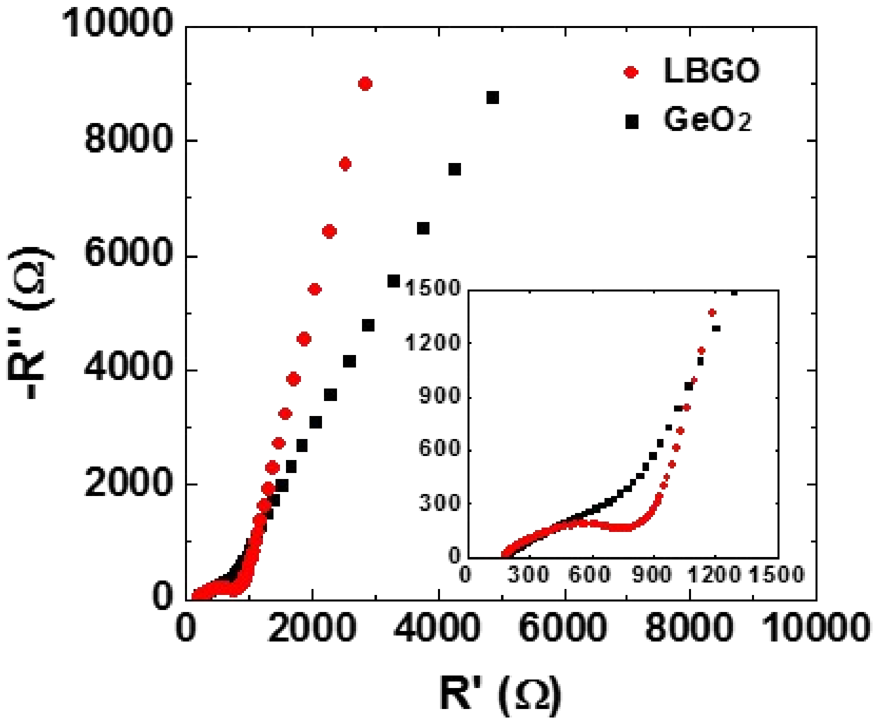

Fig. S6 Electrochemical impedance spectroscopy (EIS) spectra of the LBGO and GeO_2 electrodes before cycling.

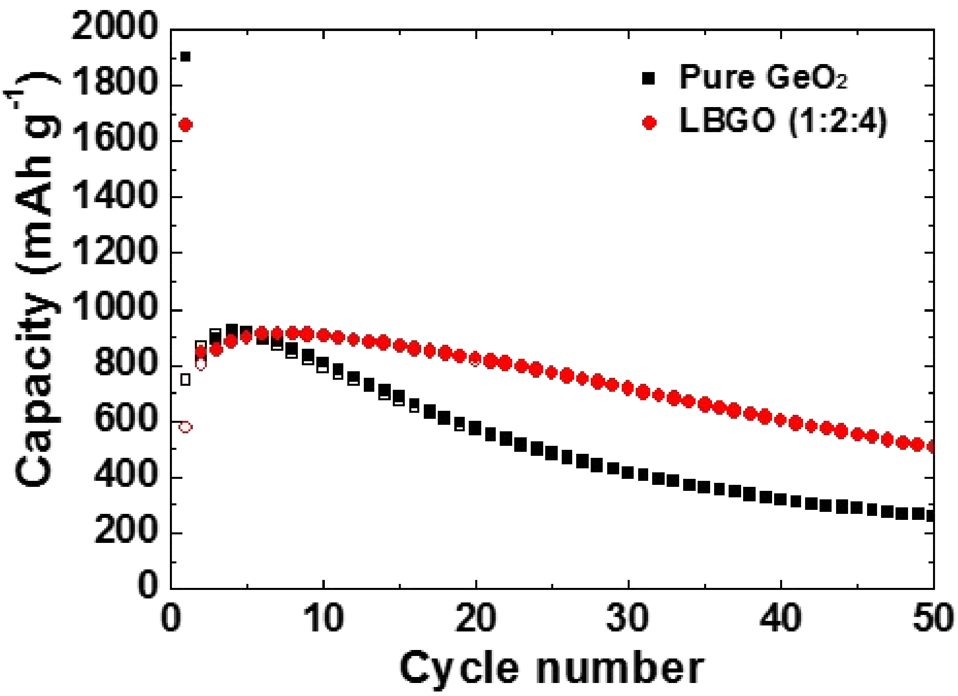

Fig. S7 Electrochemical properties of the GeO_2 and Li_2O-$2B_2O_3$-$4GeO_2$ electrodes at a constant current density of 1 A g^{-1}.